Available online at www.sciencedirect.com
SCIENCE DIRECT®
ELSEVIER
European Journal of Mechanics B/Fluids 23 (2004) 189–197
EUROPEAN JOURNAL OF MECHANICS B/FLUIDS

Closed-loop control of fluid–structure interactions on a flexibly supported cylinder

M.M. Zhang, L. Cheng *, Y. Zhou

Department of Mechanical Engineering, The Hong Kong Polytechnic University, Hung Hom, Kowloon, Hong Kong

Received 21 March 2003; accepted 29 May 2003

Abstract

This work proposes a closed-loop control of vortex-induced vibrations on a flexibly supported square cylinder. One side of the cylinder was perturbed using actuators, which were controlled by a proportional-integral-derivative controller with its feedback signal provided by a hot wire placed in the near wake. The particle image velocimetry, hot wire and laser vibrometer measurements indicate that the perturbation has completely modified the fluid–structure interaction, drastically impairing the resonance between vortex shedding and vortex-induced structural vibration. Compared with an open-loop control, the closed-loop control has two advantages. Firstly, the perturbation amplitude required to suppress vortex shedding/structural vibration is reduced by about 70%. Secondly, the closed-loop control always suppresses vortex shedding/structural vibration, while an open loop may, or may not, depending on the relationship between the vortex shedding and perturbation frequencies.

Keywords: Vortex-induced vibration; Closed-loop control; PID controller; Wake

1. Introduction

Because of its engineering significance, the control of vortex-induced vibration on bluff bodies in a cross flow has attracted a great deal of attention in the literature. The control can be passive or active. The former frequently relies on adding surface protrusions, shrouds or near-wake stabilizers to the structures to modify vortex shedding [1], while the latter involves the input of energies via activating elements called "actuators" to achieve the desired changes of a system. With the advent of new functional materials and fast developing digital processing and control technology, active control has nowadays become a hot research topic. An excellent review of previous work on active flow control can be found in Gad-el-Hak [2].

The active control may be an open or closed loop, depending on whether a feedback signal is deployed. Cheng et al. [3] recently proposed a novel technique to control the synchronization of vortex shedding with vortex-induced structural vibration. Piezoelectric ceramic actuators, embedded underneath the surface of a square cylinder, were used to create a local perturbation on the surface of the cylinder. This perturbation, without a feedback signal, was apparently an open-loop control and was found to be very effective in suppressing vortex shedding and structural vibration when the actuating signal was properly tuned in terms of frequency. However, the open-loop control suffers from a number of drawbacks. First, the perturbation amplitude of the actuators had to be reasonably large, about 2.8% of the square cylinder height or 25% of the vibration amplitude of the cylinder. Second, the perturbation frequency must be in a certain small range to achieve the best performance. A slight change in the perturbation frequency could result in a deteriorated performance or even opposite to the desired effect.

It is of interest to investigate whether the above problems associated with an open-loop control can be resolved using a closed-loop control system. The closed-loop control has been attempted in the past based on different actuation mechanisms.

* Corresponding author.
E-mail address: mmlcheng@polyu.edu.hk (L. Cheng).

0997-7546/$ – see front matter
doi:10.1016/j.euromechflu.2003.05.005

A compendium of recent papers on the control of flow-induced structural vibrations as well as flows can be found in Cheng et al. [3]. Various techniques have been investigated, including oscillating cylinders [4–6], acoustic excitations [7–9] and surface bleeding [10]. While most of previous investigations focused on the flow control, Baz et al. [11] attempted to use electromagnetic actuators to control cylinder vibrations, where flow was considered to be a disturbance rather than a control target. In contrast, Cheng et al. [3] was an attempt to modify the interactions between synchronizing vortex shedding and structural vibration.

This work proposes a closed-loop control system and aims to overcome the drawbacks of Cheng et al.'s open-loop control system. To this end, a proportional-integral-derivative (PID) controller was used with the feedback signal provided by a hot wire placed in the near wake. The control performance was assessed based on particle image velocimetry (PIV), hot wire and laser vibrometer measurements.

2. Experimental conditions

Experiments were carried out in a closed circuit wind tunnel with a square test section of 0.6 m × 0.6 m, which is 2.4 m long. The free-stream turbulence intensity is less than 0.4%. Readers are referred to Zhou et al. [12] for more details of the tunnel. The test cylinder was the same as used in [3]. A square cylinder of height $h = 15.2$ mm, flexibly supported on springs at both ends, was placed 0.2 m downstream of the exit plane of the contraction and allowed to vibrate laterally (Fig. 1). Measurements were conducted at a free-stream velocity $U_\infty = 3.58\ \mathrm{m{\cdot}s^{-1}}$, when the resonance occurred, that is, the vortex shedding frequency, f_s, synchronized with the natural frequency, f_n' (=30 Hz), of the cylinder system. The corresponding Reynolds number, Re ($\equiv U_\infty h/\nu$, where ν is the kinematic viscosity), was 3500, and the maximum oscillating displacement of cylinder, $Y_{\max}$, was about 1.2 mm, or $0.08h$.

The upper side, parallel to the flow, of the cylinder was made of a thin plastic plate (13.8 mm × 493 mm, 2/3 of the cylinder length) of 3 mm thickness, which was installed symmetrically about the mid span of the cylinder and flush with the rest of the cylinder surface. Three curved piezoelectric ceramic actuators were embedded in series in a slot underneath the plate. When placed within an electric field, the piezoelectric effect results in a strain in material. Under an applied voltage, the actuator deforms out of plane, and the thin plate moves up and down, giving the desired surface perturbation. More details about the installation and characteristics of the actuators can be found in [3].

The structural displacement, Y, was measured using a Polytec 3000 Dual Channel Laser vibrometer at a point on the unperturbed part of the cylinder surface. Two 5 μm Tungsten hot wires, operated on a constant temperature anemometer at

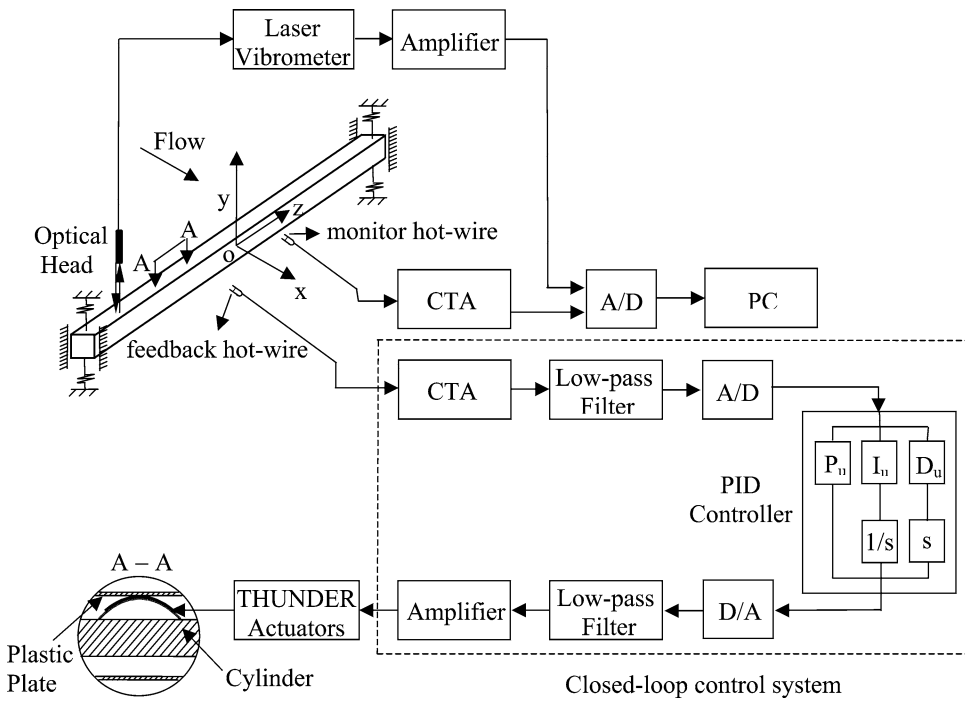

Fig. 1. Experimental setup.

an overheat ratio of 1.8, were used to monitor the streamwise velocity fluctuations, u. One hot wire, placed at $x/h = 1.6$ and $y/h = -2.5$, acted as a sensor providing a feedback signal to the controller, and the other was placed at $x/h = 2$ and $y/h = 1.5$ to monitor the velocity fluctuation. Here, x and y are the downstream and lateral distance from the cylinder center (Fig. 1). The location of the sensor hot wire certainly affects the control performance. In the present case, the sensor hot wire is located within the turbulent near-wake region ($x < 3h$) behind the cylinder, where vortices are highly coherent. The feedback signal was low-pass filtered at 200 Hz and digitized using a 16 bit AD converter, and then sent to a PID controller. The control signal generated by the controller was amplified by a piezo driver amplifier (Trek PZD 700) to activate the actuators. Both laser vibrometer and hot wire signals were conditioned and digitized using a 12-bit AD board at a sampling frequency of 3.5 kHz per channel. The duration of each record was about 20 s.

The flow field was measured using a DANTEC particle image velocimetry (PIV) system. The flow images were taken by a CCD camera (HiSense type 13, gain $\times$ 4, double frames, 1280 $\times$ 1024 pixels) and the illumination was given by two New wave standard pulsed laser sources of a wavelength of 532 nm, each having a maximum energy output of 120 mJ. A Dantec FlowMap Processor (PIV2100 type) was used to synchronize image taking and illumination. A wide-angle lens was used so that each image covered an area of 155 mm $\times$ 140 mm of the flow field, i.e., $x/h \approx 0.6$–10.8 and $y/h \approx -4.8$–4.4.

3. PID controller and parameter tuning

The PID control is a relatively matured technique, which has been applied in a wide range of areas such as process control, motor drives and flight control, etc. The output of the controller is proportional to the input, its integral and its derivative. Each combination of the three quantities results in one control strategy. Consequently, we may have P control, PI control and PID control, etc. In the most generic case, a PID controller involves optimally setting three proportionalities, referred to as the gains of the controller. Presently a PID controller was developed and implemented on an open source software platform dSPACE. The dSPACE system is a commercial package including real-time systems for rapid control prototyping, production code generation, and hardware-in-the-loop test functions. It can significantly simplify the development processes of the controller. A digital signal processor (DSP) with the SIMULINK function of MATLAB and software (ControlDesk 2.0) was used for sampling and processing the feedback signal. The PID controller was designed to minimize simultaneously the cylinder vibration (Y) and u by manually adjusting proportional gain (P_u), integral gain (I_u) and differential gain (D_u).

Parameter tuning started with P_u. Fig. 2(a) shows the dependence on P_u of the root-mean-square value $Y_{\rm rms}$ of measured Y and $u_{\rm rms}$ of u. For $P_u < 2$, both $Y_{\rm rms}$ and $u_{\rm rms}$ exhibit large oscillations, suggesting insufficient feedback control to break the synchronizing vortex shedding and structural vibration. As P_u increases from 2 to 5.6, both $Y_{\rm rms}$ and $u_{\rm rms}$ decline steadily, reaching the minimum at $P_u = 3.5$. A further increase in P_u beyond 5.6 leads to an increasing $Y_{\rm rms}$ and $u_{\rm rms}$, reaching a maximum at $P_u \approx 7$ (not shown), which is twice the value at $P_u = 3.5$. The observation conforms to Ziegler–Nichols rules [13].

A combined P and I control, i.e., a PI controller, may suppress the steady-state error but can cause a larger transient overshoot, resulting in the possible deterioration of a dynamic response in any unsteady situations [14]. The addition of a derivative term to the PI controller, i.e., a PID controller, provides an acceptable error reduction along with acceptable stability. Thus, I_u was introduced while P_u was maintained at 3.5 (Fig. 2(b)). $Y_{\rm rms}$ and $u_{\rm rms}$ display a relatively small dependence on I_u. Evidently, an optimal control performance was obtained at $I_u = 0.2$. Adding the D control showed a modest effect on the control performance (Fig. 2(c)); an optimal D_u seems to occur at 0.0001 for $P_u = 3.5$ and $I_u = 0.2$.

It is evident that P_u plays a predominant role in the present PID control scheme. This is reasonable. Before perturbation, vortex shedding and structural vibration are synchronized, implying a strong correlation between the u and Y signals [3]. P control ensures that the control action is proportional to the feedback signal, i.e., u, thus physically implying a change in the system damping. The synchronizing vortex shedding and structural vibration system at resonance is surely very sensitive to any damping change in the system. On the other hand, the control action is proportional to displacement in I control and to acceleration in D control. The former affects stiffness, while the latter modifies mass. Both result in a slight change in the natural frequency of the fluid-cylinder system. For a bluff body with fixed flow separation points, however, the synchronizing vortex shedding and induced structural vibration are strongly coupled within a certain frequency range [15]; a slight change in the system natural frequency is unlikely to bring about any considerable effect.

When the optimal parameters, i.e., $P_u = 3.5$, $I_u = 0.2$, $D_u = 0.0001$, were used, $Y_{\rm rms}$ and $u_{\rm rms}$ were attenuated by 53% and 32%, respectively, compared with the case without perturbation.

4. Performance of the closed-loop control and discussions

Fig. 3 compares the iso-contours of the normalized spanwise vorticity, $\omega_z^* = \omega_z h/U_\infty$, from the PIV measurement for four different cases: unperturbed flow, perturbed flow (open-loop control) at a perturbation frequency $f_p^* = f_p h/U_\infty = 0.1$ and

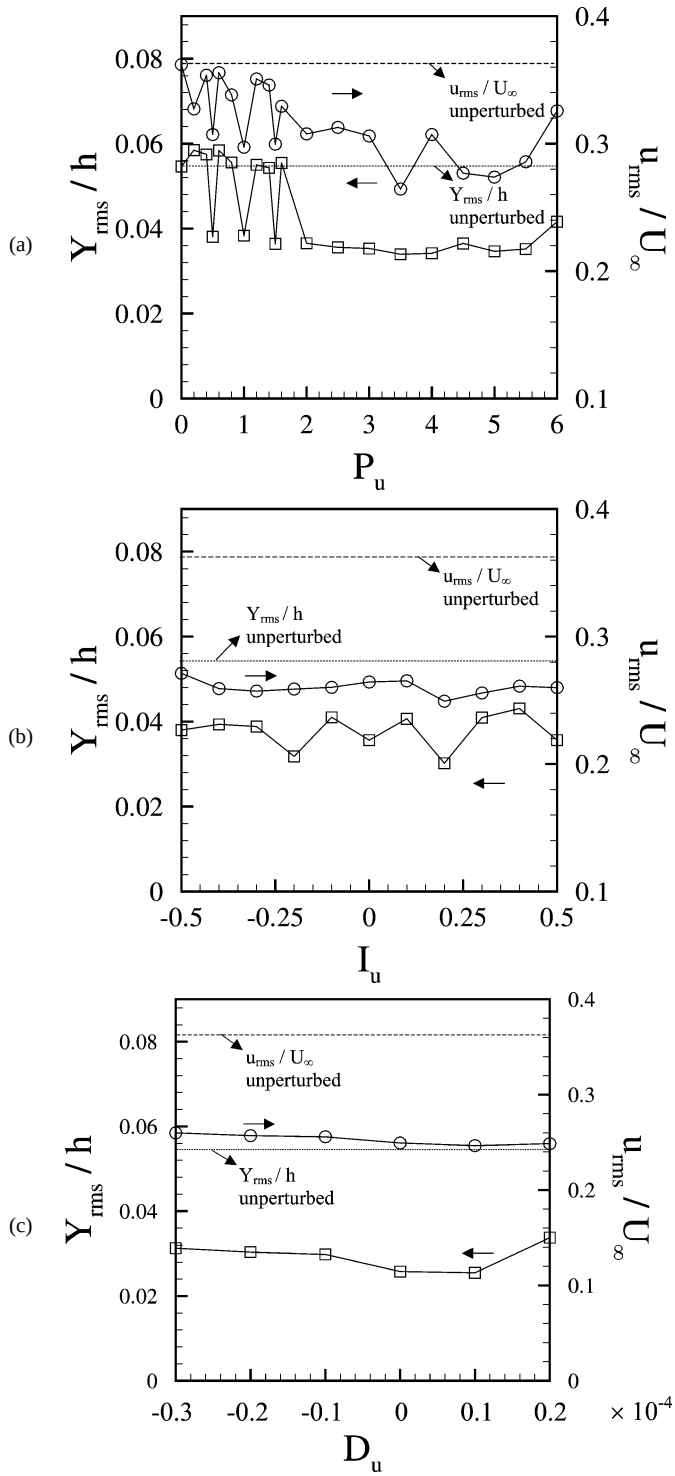

Fig. 2. Dependence of $Y_{\rm rms}/h$ and $u_{\rm rms}/U_\infty$ on proportional gain (P_u), integral gain (I_u) and derivative gain (D_u) of the PID controller. (a) The P control, $I_u = D_u = 0$; (b) the PI control, $P_u = 3.5$, $D_u = 0$; (c) the PID control, $P_u = 3.5$, $I_u = 0.2$. The feedback and monitoring hot wires were located at $x/h = 1.6$, $y/h = -2.5$ and $x/h = 2$, $y/h = 1.5$, respectively.

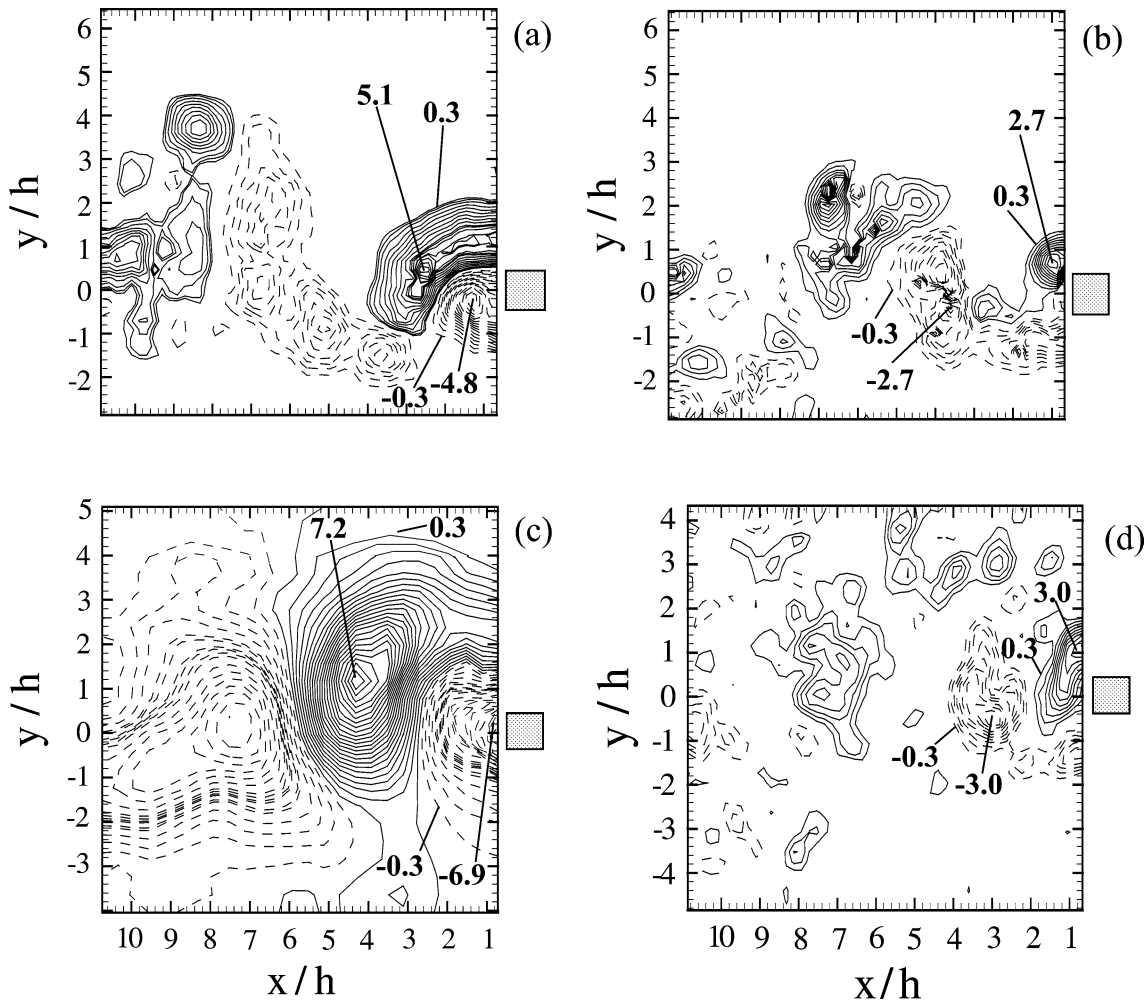

Fig. 3. The iso-contour of spanwise vorticity $\omega_z^* = \omega_z h/U_\infty$ from the PIV measurements: (a) unperturbed; (b) open-loop perturbation, $f_p^* = 0.1$; (c) open-loop perturbation, $f_p^* = 0.13$; (d) closed-loop control, $P_u = 3.5$, $I_u = 0.2$, $D_u = 0.0001$.

at $f_p^* = f_s^* = f_n'^* = 0.13$, the closed-loop controlled flow, respectively. Unless otherwise stated, the optimal parameters, i.e., $P_u = 3.5$, $I_u = 0.2$ and $D_u = 0.0001$, were used in the closed-loop control. The PIV vorticity contours presented here are instantaneous rather than phase averaged. The uncertainty of the vorticity measurement was estimated to be about 9%. The solid square in each figure indicates the cylinder position.

Without perturbation, vortex shedding synchronizes with the structural oscillation and the vorticity contours display the familiar Kármán vortex street (Fig. 3(a)). Once perturbed at $f_p^* = 0.1$, the vortex street appears to break up and becomes significantly impaired (Fig. 3(b)). The vortex circulation (Γ) can be estimated by

$$\frac{\Gamma}{U_\infty h} = \sum_{i,j} (\omega_z^*)_{ij} \frac{\Delta A}{h^2}. \tag{1}$$

In (1) $(\omega_z^*)_{ij}$ is spanwise vorticity over area $\Delta A = \Delta x \Delta y$, where Δx and Δy are the integral step along x and y directions, respectively. The cutoff level $|\omega_{zc}^*|$ was 0.3, about 7% of the maximum level, $|\omega_{z\max}^*|$, of ω_z^*, as used by Brian [16]. The Γ decrease was up to 49%, compared with the unperturbed flow. This is the best performance in suppressing the vortex street and structural vibration as f_p^* varies from 0 to 0.11. At $f_p^* = f_s^* = f_n'^* = 0.13$, however, the perturbed vortices (Fig. 3(c)) were greatly enhanced, with the maximum ω_z^* jumping by 38% and a Γ doubling that of the unperturbed flow. On the other hand, the structural oscillating amplitude climbs by 117%. Evidently, the control effect depends on the perturbation frequency. Furthermore, in the open-loop control, a relatively large perturbation amplitude is necessary for modifying the flow effectively; this amplitude was presently about 2.8%h or 25% of the cylinder oscillation amplitude.

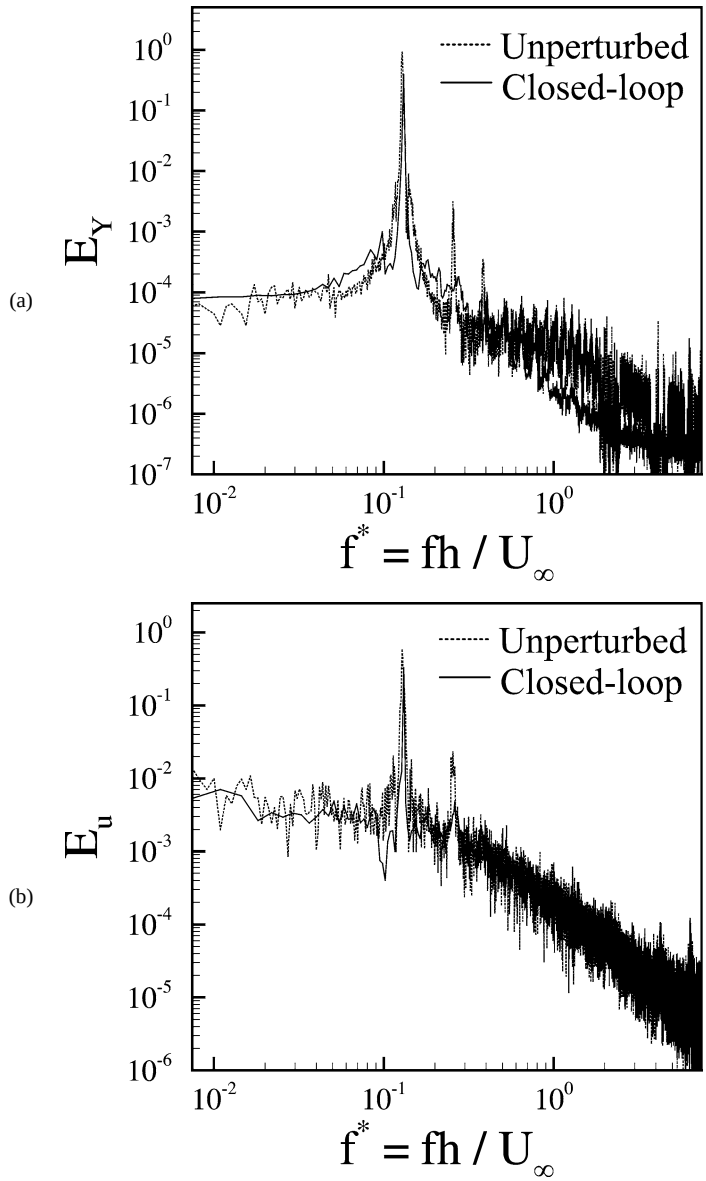

Fig. 4. Power spectra of structural vibration Y (a) and fluctuating flow velocity u (b) with and without closed-loop control. The feedback and monitoring hot wires were located at $x/h = 1.6$, $y/h = -2.5$ and $x/h = 2$, $y/h = 1.5$, respectively.

In the case of the closed-loop control, the Kármán vortex street (Fig. 3(d)) again appears to break up. The maximum vorticity drops by 41%, Γ reduces by 34%, and the structural oscillating amplitude declines by 53%, compared with the unperturbed flow. The performance is similar to the case of the best performed open-loop control at $f_p^* = 0.1$ (Fig. 3(b)). The required perturbation amplitude was, however, only 0.9%h or 8% of the cylinder oscillation amplitude, that is, one third of the amplitude (or control voltage on the actuators) required by the open-loop control.

It is of interest to understand how the closed-loop control modifies the fluid–structure interactions, which may provide insight into the physics behind the greatly weakened cylinder oscillation and vortex street. Fig. 4 presents the power spectra, E_Y and E_u, of Y and u, both normalized so that $\int_0^\infty E_\alpha(f)\,\mathrm{d}f = 1$, where α represents either Y or u. Without perturbation, both E_Y and E_u display a pronounced peak at $f_s^* = 0.13$, coinciding with the frequency of vortex shedding from a square cylinder [17–19]. The second and even the third harmonic peaks are also evident at $f^* = 0.26$ and 0.39, respectively. Once the closed-loop control is applied, the pronounced peak in both E_Y and E_u at f_s^* falls off sharply by 57% and 44%, respectively.

Meanwhile, the peaks at higher-order harmonics are also attenuated, conforming to the observation from the PIV measurements that the vortex street is by and large destroyed due to the perturbation (Fig. 3(d)).

The interrelationship between the fluid and structure interactions may be provided by examining the spectral phase shift (ϕ_{Yu}) between Y and u (Fig. 5), defined by $\phi_{Yu} = \tan^{-1}(Q_{Yu}/\mathrm{Co}_{Yu})$, where Co_{Yu} and Q_{Yu} are the cospectrum and quadrature spectrum of Y and u, respectively. The spectra were computed from a fast Fourier transform scheme as used by Zhang et al. [20]. For the unperturbed flow, ϕ_{Yu} is about zero over a small range of frequencies around $f^* = f_s^* = 0.13$.

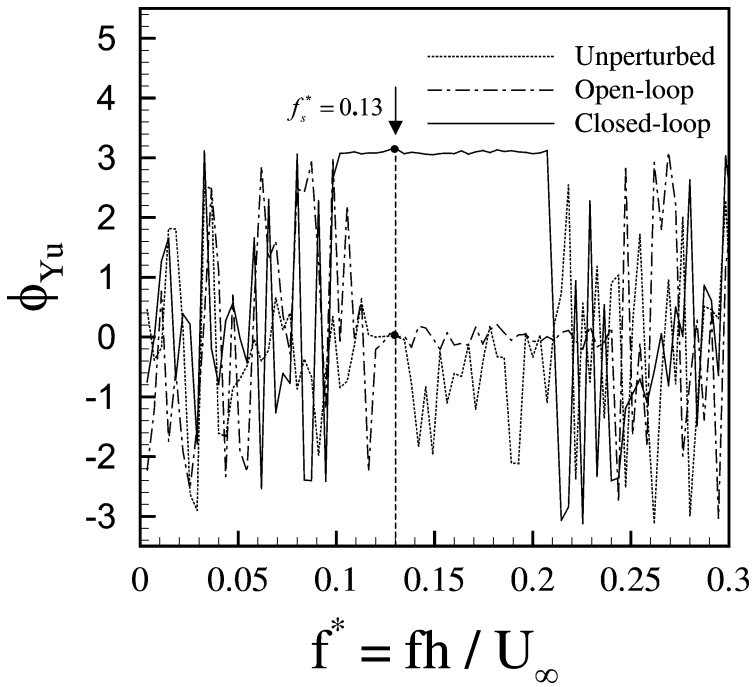

Fig. 5. Spectral phase shift ϕ_{Yu} between structural vibration Y and fluctuating flow velocity u signals with and without control. The feedback and monitoring hot wires were located at $x/h = 1.6$, $y/h = -2.5$ and $x/h = 2$, $y/h = 1.5$, respectively.

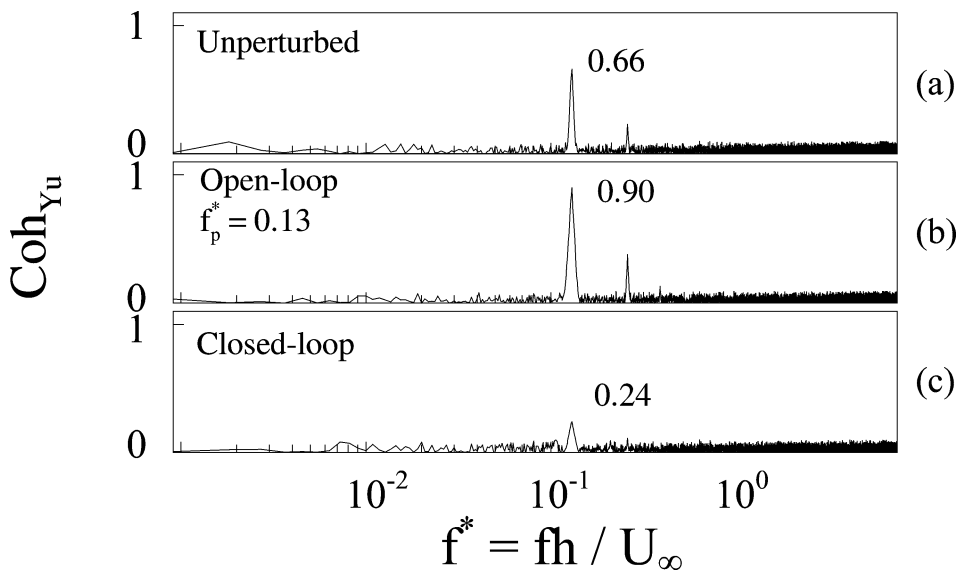

Fig. 6. Spectral coherence Coh_{Yu} between structural vibration Y and fluctuating flow velocity u with and without control. The feedback and monitoring hot wires were located at $x/h = 1.6$, $y/h = -2.5$ and $x/h = 2$, $y/h = 1.5$, respectively.

As discussed in detail in [3], ϕ_{Yu} may in effect represent the phase relation between the lateral velocity, v, of the flow and the structural oscillating velocity, $\dot{Y}$, that is, $\phi_{Yu} = 0$ corresponds to the synchronizing movement between vortex shedding and structural oscillation. Expectedly, the spectral coherence, $\mathrm{Coh}_{Yu} = (\mathrm{Co}_{Yu}^2 + Q_{Yu}^2)/E_Y E_u$, which provides a measure of correlation between Y and u, displays a pronounced peak at $f^* = f_s^*$, amounting to 0.66 (Fig. 6(a)).

For the open-loop perturbation at $f_p^* = 0.13$, the synchronizing movement is enhanced, as indicated by the expanded zero-phase frequency range. The corresponding Coh_{Yu} climbs to 0.90 at $f^* = 0.13$ (Fig. 6(b)). For bluff bodies with fixed separation points, Gowda [15] reported that the synchronization or lock-in between vortex shedding and its induced vibration began at $f_s \approx 0.8 f_n'$ and ended at $f_s \approx 2 f_n'$, corresponding to a present frequency range of $f^* = 0.11$–0.26. The zero-phase frequency at $f_p^* = 0.13$ ranges between $f^* = 0.12$ and 0.24, almost coinciding with the possible lock-in range reported by Gowda. Once the perturbation frequency of an open-loop perturbation does not fall in this lock-in range, the synchronizing movement between vortex shedding and structural oscillation may be altered; for example, the open-loop perturbation at $f_p^* = 0.1$ resulted in $\phi_{Yu} \approx \pi$ in a narrow range centered at $f^* = 0.13$ (see Fig. 17 in [3]).

In the closed-loop control case, ϕ_{Yu} (Fig. 5) changes from 0 to about π over a wide frequency range of $f^* = 0.10$ to 0.21, implying that the structural and fluid motions are now in anti-phase. The interrelationship between v and $\dot{Y}$ changes from reinforcing each other to acting against each other. As a result, the correlation between vortex shedding and structural motion is drastically reduced, as evidenced by the declining maximum Coh_{Yu} to 0.24 at $f^* = f_s^*$ (Fig. 6(c)), and both the structural vibration amplitude and vortex strength are greatly reduced (Figs. 2–4).

5. Conclusions

This paper presents an attempt to control vortex shedding and vortex-induced vibration on a square cylinder in cross flow using the closed-loop PID controller. The investigation leads to the following conclusions.

1. Among three gains used in the PID controller, P control, which physically adds damping to the fluid–structure system, is shown to be most effective, compared with I and D controls, which physically influence the stiffness and mass of the system, respectively.
2. The closed-loop PID control has successfully altered the nature of coupling between the synchronizing vortex shedding and vortex-induced structural oscillation, thus suppressing both vortex shedding and structural vibration. In contrast, the open-loop control of the present surface perturbation technique can only suppress vortex shedding or vortex-induced vibration provided that the perturbation frequency does not fall within the synchronization range of vortex shedding and structural oscillation.
3. The closed-loop control requires a minimum perturbation amplitude, about one third of that required by the open-loop control given the same surface perturbation technique, making it possible to develop a more compact, self-contained and low energy control system.

Acknowledgements

The authors wish to acknowledge support given to them by the Research Grants Committee of The HKSAR (Grant no. PolyU 5294/03E).

References

[1] M.M. Zdravkovich, Review and classification of various aerodynamic and hydrodynamic means for suppressing vortex shedding, J. Wind Eng. Ind. Aerod. 7 (1981) 145–189.
[2] M. Gad-el-Hak, Flow control: the future, J. Aircraft 38 (2001) 402–418.
[3] L. Cheng, Y. Zhou, M.M. Zhang, Perturbed interaction between vortex shedding and induced vibration, J. Fluids Structures 17 (2003) 887–901.
[4] N. Fujisawa, Y. Kawaji, K. Ikemoto, Feedback control of vortex shedding from a circular cylinder by rotational oscillations, J. Fluids Structures 15 (2001) 23–37.
[5] E. Berger, Suppression of vortex shedding and turbulence behind oscillating cylinders, Phys. Fluids 10 (1967) 191–193.
[6] H.M. Warui, N. Fujisawa, Feedback control of vortex shedding from a circular cylinder by cross-flow cylinder oscillations, Exp. Fluids 21 (1996) 49–56.
[7] J.E. Ffowcs Williams, B.C. Zhao, The active control of vortex shedding, J. Fluids Structures 3 (1989) 115–122.
[8] K. Roussopoulos, Feedback control of vortex shedding at low Reynolds numbers, J. Fluid Mech. 248 (1993) 267–296.

[9] X.Y. Huang, Feedback control of vortex shedding from a circular cylinder, Exp. Fluids 20 (1996) 218–224.
[10] M.D. Gunzburger, H.C. Lee, Feedback control of Karman vortex shedding, Trans. ASME J. Appl. Mech. 63 (1996) 828–835.
[11] A. Baz, J. Ro, Active control of flow-induced vibrations of a flexible cylinder using direct velocity feedback, J. Sound Vib. 146 (1991) 33–45.
[12] Y. Zhou, H.J. Zhang, M.W. Liu, The turbulent wake of two side-by-side circular cylinders, J. Fluid Mech. 458 (2002) 303–332.
[13] J.G. Ziegler, N.B. Nichols, Optimum settings for automatic controllers, Intech 42 (1995) 94–100.
[14] M. Driels, Linear Control Systems Engineering, McGraw-Hill, New York, 1996.
[15] B.H.L. Gowda, Some measurements on the phenomenon of vortex shedding and induced vibrations of circular cylinders, Deutsche Luft- und Raumfahrt Forschungsbericht, No. 75-01, 1975.
[16] C. Brian, C. Donald, An experimental study of entrainment and transport in the turbulent near wake of a circular cylinder, J. Fluid Mech. 136 (1983) 321–374.
[17] B.J. Vickery, Fluctuating lift and drag on a long cylinder of square cross-section in a smooth and turbulent stream, J. Fluid Mech. 25 (1966) 481–494.
[18] D.A. Lyn, W. Rodi, The flapping shear layer formed by flow separation from the forward corner of a square cylinder, J. Fluid Mech. 267 (1994) 353–376.
[19] Y. Zhou, R.A. Antonia, Memory effects in turbulent plane wakes, Exp. Fluids 19 (1995) 112–120.
[20] H.J. Zhang, Y. Zhou, R.A. Antonia, Longitudinal and spanwise structures in a turbulent wake, Phys. Fluids 12 (2000) 2954–2964.